



Structure and antibacterial activity of PLA-based biodegradable nanocomposite coatings by electron beam deposition from active gas phase

Chun He^a, Qi Chen^a, M.A. Yarmolenko^{a,b,*}, A.A. Rogachev^{a,b}, D.G. Piliptsov^{a,b}, Xiaohong Jiang^{a,**}, A.V. Rogachev^{a,b}

^a International Chinese-Belorussian Scientific Laboratory on Vacuum-Plasma Technology, College of Chemical Engineering, Nanjing University of Science and Technology, Nanjing 210094, China

^b Francisk Skorina Gomel State University, 104, Sovetskaya Street, Gomel 246019, Belarus

ARTICLE INFO

Keywords:

Electron-beam deposition

PLA

AgNPs

Norfloxacin

Antibacterial activity

ABSTRACT

The synthesized poly(lactic acid)-based (PLA-based) biodegradable nanocomposite coatings with antibacterial properties were prepared from active gas phase generated by low-energy electron beam dispersion of the powder mixture of PLA and antibacterial components (Norfloxacin and silver nitrate, respectively) in vacuum. The molecular structure, morphology, optical property and chemical states of PLA-based coatings were investigated by ATR-FTIR, UV-Vis, TEM and XPS. The analyses of ATR-FTIR spectra confirm the formation of polymer and the doped antibacterial components and show the interaction between them. XPS data show that the Ag nanoparticles are of metallic nature in the case of PLA-based nanocomposite coatings containing silver. The antibacterial activity of PLA-based coatings deposited on different substrates was tested against *E. coli* ATCC 25922 and *S. aureus* ATCC 12600 using the agar diffusion method on the solid LB agar medium. The influence of substrates on their antimicrobial behavior was stated.

1. Introduction

Advanced implant associated biomedical technologies for open fracture treatments including biomedical implants and devices have experienced a stage of rapid boom and found their practical implementations in improving the quality of human and animal lives within the last few decades. While building up health conditions of patients, possible subsequent implant related postoperative infections have become critical health concerns and perhaps the trickiest infections to conduct [1–4]. The treatment of postsurgical infections always requests prolonged therapy of antibiotics and might even lead to a possible removal of the placed internal devices through orthopedic surgeries [5]. In severe cases, an amputation may be needed which can lead to the death of patients in the worst cases. In the process of infection formation, the initial crucial step is the adhesion and anchorage of bacteria on the surface of implants and biomaterials. Bacterial adhesion occurs due to the attachment of them to the surface of biomedical devices followed by a slow colonisation of the bacteria and subsequently leads to the formation of a bacterial biofilm which is fatal for the development of infection. Therefore, the suppression of biofilm

formation is a significant challenge towards prophylaxis and reduction of implant related infections. Concerning the bacterial adhesion, which is determined by the properties of implant surface, much effort has been attributed to modify it with biodegradable materials, since they will be used in biomedical industry.

Biodegradable polymeric materials which are blood compatible have been applied not only confined to biomedical implants and devices [1,6], release of drugs [7–9], food packagings [10,11], but also extended to wound dressings [12], bone cements [13] and tissue engineering scaffolds [14–16] due to their environment friendly nature and outstanding physicochemical features. One key reason that makes them attractive and interesting is their capacity of total biodegradability. The most well-known and important aliphatic poly(lactic acid) (PLA) and poly(glycolic acid) (PGA) of polymer family or their copolymers have been the most investigated biodegradable materials which are widely occupied as surgical products and biodegradable implants [17,18]. They have played a predominant role as biodegradable materials in orthopedic and medical applications, and among them the renewable biodegradable PLA has drawn the most attention and interest owing to its remarkable properties that make its commercial and

* Corresponding author at: International Chinese-Belorussian Scientific laboratory on Vacuum-Plasma Technology, College of Chemical Engineering, Nanjing University of Science and Technology, Nanjing 210094, China.

** Corresponding author.

E-mail addresses: simmak79@mail.ru (M.A. Yarmolenko), jxh0668@sina.com (X. Jiang).

<https://doi.org/10.1016/j.porgcoat.2018.02.030>

Received 17 September 2017; Received in revised form 9 January 2018; Accepted 27 February 2018

0300-9440/© 2018 Elsevier B.V. All rights reserved.

large-scale production suitable for a large range of utilizations [19,20].

The modification of implant surfaces aiming at preventing infections can be conveniently achieved by coating the implant with nanocomposite antibacterial thin coatings loaded with antibiotics or other antimicrobial agents. The application of antibiotics constitutes a key point for the prophylaxis of implant related infections. It is well known that Norfloxacin is one of the most efficient antibiotics for preventing infections in hospitalized patients due to its excellent antimicrobial performance. The presence of antibiotics has a vital influence on bacterial adhesion and proliferation on the implant surface. Therefore, polymer-antibiotic coatings have been considered as one of the most promising and appealing options for treatment of implant related infections as these coatings will release antibiotics from implant surface to the internal environment, and as a result the production of medical implants coated with polymer-antibiotic coatings is highly demanded [6].

Silver nanoparticles (AgNPs) have been suggested to be the most promising inorganic nanoscale antimicrobial agents and broadly employed in precaution of implant related infections in medical sector due to their powerful antibacterial capacity against a great number of microorganisms. Hence, the antibacterial property of AgNPs has aroused a great interest of researchers and been considerably discussed [21,22]. It has been substantiated that the high surface area to contact of AgNPs is responsible for the enhanced inhibitory activity of nanomaterials. However, on the other hand, the high surface free energy of AgNPs also endows them with a tendency to be aggregated and oxidized when they are in contact with environment which may result in the decrease or even loss of some of their particular features. One commendable way to solve these problems is to introduce nano-sized Ag particles into stable polymer matrix materials to protect them from undergoing aggregation and oxidation which may retain their antibacterial property to some extent [15,23].

In most traditional preparation methods of polymer-based nanocomposite coatings with low-molecular compounds or metallic nanoparticles as doped components, there always are liquid media or solvents. As a result, these methods usually have restrictions to the range of polymer matrixes and dispersed substances, the rate of deposition and the thickness of the synthesized coatings. One possible way to effectively overcome these drawbacks and get rid of solvents is the solvent-free low-energy electron beam coating deposition method in vacuum. The electron beam deposition method allows combining the advantages of both physical vapor deposition (PVD) methods and chemical vapor deposition (CVD) methods [24–26]. Specifically, the polymer-based nanocomposite thin coatings are deposited from the active gas phase generated as the products of electron beam dispersion of the solid target consisting of composite polymer based substances. In our case, the low-energy electron beam flux can effectively evaporate and further disperse the powder mixture of polymer and doped components and give rise to the formation of even and dense nanocomposite coatings in company with the uniform distribution of dispersed low-molecular compounds or metallic nanoparticles in polymer matrix volume. The deposition of coatings based on many high-molecular compounds: polytetrafluoroethylene, polyethylene, polyurethane, polyaniline, silicone resins, etc. and nanocomposite coatings on their basis are possible by electron beam dispersion. The deposition of these coatings, in particular, PU-PTFE, PE-PTFE by other methods is difficult or impossible [27]. Electron beam dispersion cannot be used for coatings based on compounds containing benzene rings (polystyrene, polyethylene terephthalate). Benzene rings are easily split off and removed by a vacuum pumping system. Electron beam dispersion is not effective in the formation of layers based on antibiotics, characterized by molecular mass of more than 800: polymyxins, vancomycin, and a number of other antibiotics – gentamycin, etc. The electron-beam coating method is most effective in the formation of layers based on ciprofloxacin. The impact of a low-energy electron flux is not accompanied by the destruction of an antibacterial drug [28,29]. Electron-

beam dispersion of high-molecular compounds is accompanied by the deposition of layers with significantly lower molecular mass, which facilitates their relatively rapid decomposition in the human body. This also applies to polylactide-based coatings. In [30] it is noted that the amorphous structure of polylactide-based coatings, combined with a low molecular weight ($9.6 \cdot 10^4$ g/mol for the initial polymer and $1.5 \cdot 10^4$ g/mol for the coating), promotes the accelerated release of biocidal additives. As is known, one of the disadvantages of polylactide materials is the low rate of biodegradation, which requires the implementation of additional techniques. In particular, the introduction of a magnesium polymer [31]. Antibacterial coatings based on polylactide are free from this disadvantage.

It should be noted then the effectiveness of using antibacterial coatings is in some cases determined by the rate (character) of the medicinal component release from the thin layer. The release of silver nanoparticles is only possible at the decomposition of the polymer layer [32]. Consequently, these coatings will have a high surface bacterial activity. Using an antibacterial chemical might expect its more intense diffusion from the coating to the biological medium. In this regard, it was interesting to compare such coatings with various release kinetics.

The aim of this study is the investigation of the antibacterial activity of PLA-based biodegradable nanocomposite coatings due to the changes in structure and morphology of the coatings under the influence of the doped antibacterial components of different nature.

2. Experiment

2.1. Characterization of methods and instruments

The nanocomposite coatings were formed by the electron beam deposition method (EBD). The mechanical mixture of powders of the polymer (poly(lactic acid), Purac) and antibacterial components (Norfloxacin, Zhejiang Medicine Co., Ltd., silver nitrate (AgNO_3), 98%, Aldrich) was taken as the initial target.

The nanocomposite coating deposition was performed from active gas phase generated in vacuum as the product of electron-beam dispersion of powder mixture of PLA and antibacterial components in the mass ratio of 1:1. The scheme of electron beam deposition device is shown in Fig. 1.

The process of nanocomposite coating deposition was carried out at the initial pressure of residual gases in the vacuum chamber at 4×10^{-3} Pa. The electron gun with a filamentary cathode which is able to form low-energy electron beams with current density $j = 0.01\text{--}0.03$ A/cm² and energy $E = 1000\text{--}2000$ eV is used as the

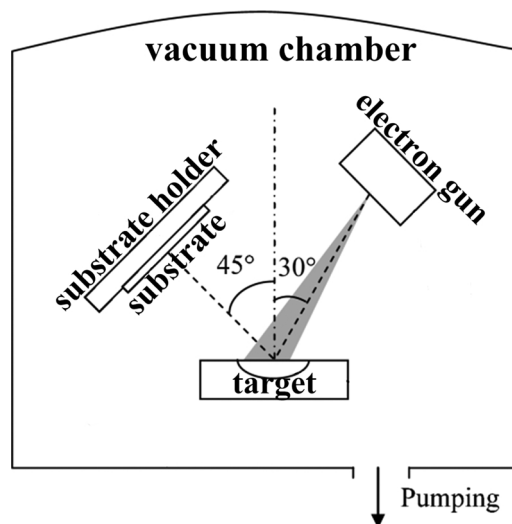


Fig. 1. Scheme of electron beam deposition device.

electron source. The distance between target and electron gun was 20 cm and between the target and substrates was 15 cm. The substrates were not exposed to energetic elastically scattered electrons. Otherwise, such a treatment would initiate a process of partial destruction of the deposited organic layer. The temperature of substrates while depositing thin layers was about 25 °C. The type of low-energy electron devices which are used to obtain polymer-based coatings in vacuum is as shown in [24,33].

Dimensional morphological analysis of nanoparticles in the polymer matrix was carried out using high resolution transmission electron microscopy (TEM) a JEM 2100 (Jeol) microscope with the acceleration voltage of 200 kV. The selection of characteristic section for the analysis was determined by the maximum number of isolated clusters. The special carbon-coated copper grid substrates were used with thin layers depositing directly onto a grid during the TEM investigations.

The molecular structure of nanocomposite coatings was characterized on the IS-10 (Thermo Scientific Nicolet) Fourier Transformed Infrared Spectrometer in a mode of attenuated total reflection (ATR). ATR-FTIR spectra were recorded in the scanning range of 4000–300 cm^{-1} with a resolution of 4 cm^{-1} . The accumulation of the signal was spent on 32 spectra and the spectrum was observed as soon as 4 spectra past.

The UV–vis spectrophotometric investigations were conducted by the Cary-50 (Varian) spectrometer using transparent quartz glasses with nanocomposite thin layers deposited on them directly. The value of the band gap was determined based on the analysis of optical absorption spectra using the methods described in [34,35].

The elemental compositions and chemical states of the deposited nanocomposite thin layers were analyzed by X-ray photoelectron spectroscopy (XPS). The XPS measurements were done on the PHI Quantera II Scannig XPS Microprobe spectrometer with Al K α monochrome X-rays ($h\nu = 1486.6$ eV) source. All the binding energies of the XPS spectra were referenced to C1s peak at 284.8 eV of the surface adventitious carbon. The pass energy of the entire XPS core spectrum is 280 eV and of the spectrum of each element is 55 eV. For PLA + AgNO $_3$ coating sample, the analysis time of the entire XPS core spectrum, C1s spectrum, N1s spectrum and Ag3d spectrum is 6.61 min, 5.42 min, 4.82 min and 3.62 min, respectively. For PLA + Norfloxacin coating sample, the analysis time of the entire XPS core spectrum is 6.51 min and of the spectrum of each element is 3.62 min. The power of charge neutralisation is 100u25w15 kV and the spot size is 200 \times 250 μm^2 .

2.2. Evaluation of antibacterial activity by the agar diffusion method

According to the analysis of literature, at the present time, several drugs that lead to a synergistic effect are used to combat pathogenic microorganisms effectively. In this regard, the combination of Norfloxacin with silver nitrate is justified. Silver nitrate is the source of silver nanoparticles, formed under the energy impact of the electron

flow, and in the heat treatment of a thin layer. It should be noted that all medical devices are thermally sterilized before being introduced into the body, which many researchers do not take into account. As a result, the coating is a source of metal nanoparticles, silver nitrate and antibacterial chemotherapy. In this case, various schemes for the thermal treatment of coated implants determine the content of the original salt in a thin layer.

The antibacterial activity of the synthesized thin layers was tested against two different pathogenic bacteria *Escherichia coli* (*E. coli* ATCC 25922, gram-negative), and *Staphylococcus aureus* (*S. aureus* ATCC 12600, gram-positive) in terms of agar diffusion method, which was conducted as previously reported in Refs. [36,37].

In order to clarify the surface antibacterial property of the formed thin coatings, the silicon single crystal wafers (100) substrates were cut prior into squares (considering it is difficult for silicon wafers to be cut into regular discs during artificial post-processing) of which each has a surface area of 10 \times 10 mm^2 besides special circular quartz glasses substrates of which each has a diameter of 10 mm with coatings deposited on them were subsequently used as the discs employed in the agar diffusion method instead of the conventional paper discs. All instruments and materials were sterilized in an autoclave before experiments. The antimicrobial activity tests for coatings prepared on these two kinds of substrates against *E. Coli* and *S. aureus* by agar diffusion method were performed on the solid Luria-Bertani (LB) agar medium at incubation temperature of 37 °C for 24 h. It has been well established that when the concentrations of inhibition are reached, there will be a formation of a clear zone around the placed sample if it is contacted with bacterial microorganisms. This clear zone is ascribed as a zone of inhibition [38]. After incubation, antibacterial activity of coating samples was determined as different levels of growth inhibition zones formed on agar plates around them which were visually observed and measured for further evaluation.

3. Results and discussion

3.1. FTIR and UV–vis spectroscopy

The molecular structure of Norfloxacin after it was fully exposed to the low-energy electron beam was measured immediately after the process of nanocomposite coatings deposition. ATR-FTIR spectrum of the Norfloxacin coating tends to be identical to spectrum of the initial Norfloxacin powder (Fig. 2(A, B)). The main absorption bands of the initial Norfloxacin powder characterized by ATR-FTIR spectroscopy appear in spectrum of Norfloxacin coating prepared from the active gas phase and negligible differences exist in the intensities of several absorption peaks between the spectra of origin powder and formed coating in spectrum frequency area 3800–2400 cm^{-1} and 1700–600 cm^{-1} . Some differences in the position and optical density of the individual absorption bands may be stipulated by the differences in

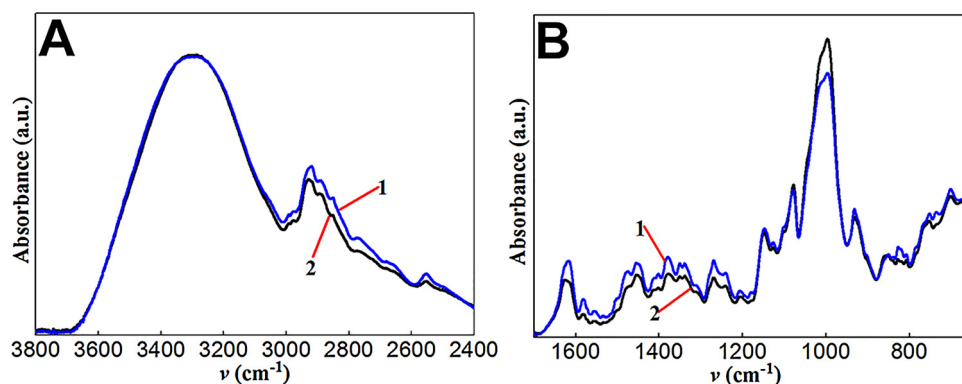


Fig. 2. ATR-FTIR spectra of the powder and coating of Norfloxacin: 1-Norfloxacin powder; 2-Norfloxacin coating.

physical state of the compound in a thin layer and the powder.

The presence of Norfloxacin is confirmed by characteristic peaks assigned to valence vibrations of its OH-, NH- groups, C-H bonds (CH₃, CH₂ and CH groups) in the range 3000–2800 cm⁻¹.

The strong and broad absorption band at 3300 cm⁻¹ can be characterized by valence vibrations of NH groups. It is known that the absorption of the secondary amine in the diluted solutions is in the range of 3500–3400 cm⁻¹. The absorption peak at 3300 cm⁻¹ may indirectly indicate the presence of intense intermolecular interactions (hydrogen bonds) involving amino groups, and the peak at 3030 cm⁻¹ can be assigned to stretching vibrations of aromatic =C-H groups of Norfloxacin [39].

The drug compound in a thin layer in the form of powder easily binds to water. This is indicated by the IR spectra through a broad absorption band in the range of 3600–3000 cm⁻¹ corresponding to stretching vibrations of OH groups, the absorption at 1650 cm⁻¹ corresponds to deformation vibrations of OH groups [25].

According to the IR spectroscopic investigations, the effect of low-energy electron beam on the drug compound is not accompanied by a noticeable degradation of its molecular structure.

Fig. 3 shows the results of UV-vis spectroscopy of PLA-based coatings. It is obvious, that the nanocomposite coatings with silver possess high activity in the visible area illustrated by a broad absorption band fixed at 415 nm which can be ascribed to the presence of AgNPs with spherical shape on the contrary to the pure PLA coating. Following two days of storage of the investigated PLA + AgNO₃ coating without taking any protective procedures, the maximum of the surface plasmon resonance absorption peak shifts to longer wavelength increasing from 415 nm to 430 nm together with the companion of an apparent broadening of the peak. The considerable broadening and shift of the peak maximum imply that the average size and distribution of AgNPs slightly increased with time [40,41]. The aggregation of AgNPs and their interface coupling effect may be the explanation for the broadening and red-shift of surface plasmon absorption [42,43]. As reported in Ref. [44], that silver particles with diameters ~10 nm exhibit absorption bands at 410–450 nm depending on their chemical environment. It is believed that small spherical nanoparticles of silver with an average diameter of 10 nm or even less are deposited into PLA coatings based on the maximal absorption at 415 nm in UV-vis spectrum. Thus, it is established that despite of the properties of polymer matrix, dispersion of the mixture of polymer and silver nitrate by electron beam is accompanied by the formation process of silver nanoparticles into polymer-based composite coatings.

In order to verify the introduction of Norfloxacin and AgNO₃ into PLA based nanocomposite coatings formed from the active gas phase, their ATR-FTIR spectra together with that of origin PLA powder were studied as presented in Fig. 4. It is worth mentioning that the thin

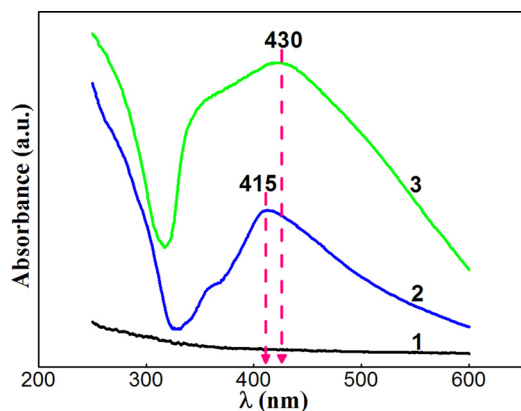


Fig. 3. UV-vis absorption spectra of the coatings: 1-PLA coating; 2-PLA + AgNO₃ coating; 3-PLA + AgNO₃ coating tested after 2 days.

coating based on silver nitrate is characterized by the absorption at 1250 and 870 cm⁻¹ due to the valence vibrations of NO₃⁻ groups and the deformation vibrations of O-N-O groups [45]. And for the investigated coating based on Norfloxacin the presence of the peaks displayed in Fig. 3 reveals the appearance of Norfloxacin structure in the composite system.

It can be seen (Fig. 4) that the IR spectra of two kinds of doped PLA based composite coatings show all the feature-distinctive absorption bands which are defined in pure PLA powder. The intense characteristic absorption peaks at 1754, 1179 and 1077 cm⁻¹ observed from the origin PLA powder shift slightly to lower wavenumber, 1712, 1235 and 1091 cm⁻¹ for PLA + AgNO₃ coating and 1740, 1185 and 1086 cm⁻¹ for PLA + Norfloxacin coating respectively, which can be attributed to C=O carbonyl stretching, stretching vibration of C-O-C groups and stretch modes of C-O groups, respectively. The absorption bands at 2982 and 2942 cm⁻¹ for PLA powder refer to stretch modes of aliphatic saturated C-H groups and asymmetric stretching vibration of C-H₂ group, respectively, appear at 2954 and 2919 cm⁻¹, 2991 and 2943 cm⁻¹, for PLA + AgNO₃ coating and PLA + Norfloxacin coating system correspondingly.

So, the IR spectra of composite coatings are represented by all the bands peculiar to the initial components. The emergence of other bands was not identified. This indicates the lack of chemical bonds occurrence between the components. As a first approximation, the coatings may be regarded as superfine mechanical mixtures of the modified original components. The shift in the bands is caused by the classical intermolecular interaction of the polymer and a low-molecular compound. In particular, for PLA - Norfloxacin coating, it is hydrogen interaction between the oxygen of oxygen-containing groups of the polymer (carbonyl, ester bonds) and the hydrogen of secondary amides of the chemical, etc. For PLA-AgNO₃ coating, in addition to the interaction between the polar groups of the polymer and salt (NO₃⁻), it is the interaction between the polymer and the formed silver nanoparticles. The result of this interaction are the processes of partial oxidation, formation and growth of silver nanoparticles. The mechanism of influence of the polymer matrix containing oxygen polar groups on the processes of the formation and growth of silver nanoparticles are described in the literature well enough today [32].

3.2. TEM studies

TEM and HRTEM images of silver containing PLA-based composite coatings synthesized by dispersion of powder mixture of AgNO₃ and PLA are shown in Fig. 5. TEM images demonstrate that many nanoparticles are fine uniformly anchored on the light-colored polymer matrix. We find that the vast majority of AgNPs have diameters from 5 to 20 nm and the average diameter of them can be determined to be 17.5 ± 1.13 nm (Fig. 5C) considering them as spherical nanoparticles which well corresponds to UV-vis results. The presence of several silver nanoclusters with the maximum size (< 200 nm) should be because of the oxidation and aggregation of silver particles on the surface of coatings in the air. Such wide range of the distribution of size and shape of AgNPs may be due to the nature of used polymer matrix. Since PLA is a kind of more active polymer as opposed to inert polymers like PTFE and PE, the interaction between silver and polymer is significant and occurred in the process of initial target impact by electron beam, subsequent active gas phase generation and deposition on a substrate and then leads to the formation of AgNPs with widened distribution of size and shape [26]. The interaction of silver nanoparticles with a polymer matrix was touched upon in [32]. It is noted that metal ions can interact with oxygen-containing groups. It was found that the decomposition of silver nitrate is accompanied by the presence, in addition to metallic nanoparticles, of oxide particles. The interaction of metal nanoparticles with an organic matrix is specified by the high surface energy of the nanoparticle. Particles of silver oxide interact with organic molecules by means of oxygen of the oxide layer.

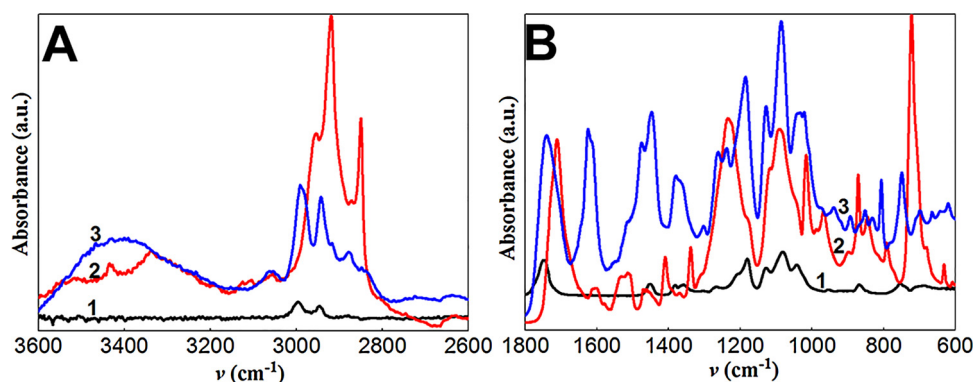


Fig. 4. ATR-FTIR spectra of coatings and PLA powder: 1-PLA powder; 2-PLA + AgNO₃ coating; 3-PLA + Norfloxacin coating.

It is clear that the observed crystal lattice spacing of single nanoparticle marked out in Fig. 5B is 0.234 nm, which is in good agreement with the value of the (111) phase of metallic Ag nanoparticles, suggesting AgNPs have successfully deposited into polymer matrix of PLA + AgNO₃ nanocomposite coatings and also confirming the conclusions drawn in data analyses of the visible area in UV–vis absorption spectra [46–48]. The existence of metallic Ag⁰ is further demonstrated in XPS spectrum (as shown in Fig. 6C).

3.3. XPS studies

The XPS core spectrum of PLA + AgNO₃ coating sample and the typical high-resolution XPS spectra of C1s and Ag3d core levels of it are shown in Fig. 6. The entire core XPS spectrum in Fig. 6A clearly indicates that elements of C, O and Ag are detected in PLA + AgNO₃ coating. No peaks of other impurities were detected in the sample, proving the resulting coating possesses high purity.

As can be seen from Fig. 6B, C1s spectrum can be deconvoluted into three peaks at 283.7 eV, 285.7 eV and 287.7 eV, which can be ascribed to aliphatic methyl –CH₃ groups, aliphatic tertiary carbon atoms bonded to oxygen atoms (O–C–H) and aliphatic C=O double bonds, respectively. The O1s spectrum is not displayed because the content of O from XPS result is not accurate to some extent. The O1s spectrum contains the contributions from surface adsorbed multiple oxygen ions, including O₂, H₂O, chemisorbed oxygen (OH) and carbonate substances during the process of sample preparation for XPS measurement which are very much common at room temperature in the air.

It is illustrated that there are two adjacent peaks centered at

373.5 eV and 367.5 eV in Ag3d photoelectron regions for PLA + AgNO₃ coating sample in Fig. 6C, which correspond to Ag3d3/2 and Ag3d5/2, respectively [49–51]. No peak corresponding for N 1s is observed, it confirm that AgNO₃ had already decomposed. Therefore, the XPS results further verify the existence of zerovalent silver Ag⁰ in the PLA-based nanocomposite coatings containing silver and support for this conclusion of the metallic nature of Ag come from TEM, which shows crystal lattice spacing of 0.234 nm that can be indexed to the (111) phase of AgNPs combined with characteristic plasmon peaks of metallic silver at about 415 nm and 430 nm in UV–vis spectra.

It should be marked out that in comparison with the standard value of pure metallic Ag, the binding energy value of bulk Ag is about 368.2 eV which is well established in the literature sources, the XPS peak position referenced to Ag3d5/2 of metallic Ag somewhat exhibits small negative shift about 0.7 eV to lower binding energy in the case of PLA + AgNO₃ thin coating in our work, implying that the electron density of Ag is decreased. The difference could be resulted from the binding energy of silver which is highly sensitive to the external environment in which it is located and in this case the polymer matrix network should be responsible for the small shift [40,52–54]. Probably the intense interaction between silver which is introduced into PLA polymer and the electronegative oxygen atoms exists in PLA polymer network, generating a consequent slight deformation of electron density from silver atoms towards the electronegative atoms, giving rise to the above mentioned shift in BE value of silver to lower binding energy.

The mechanism of interaction between the positively charged silver ions and oxygen-containing groups of the polymer that have negative charge is well described in the literature. These photochemically

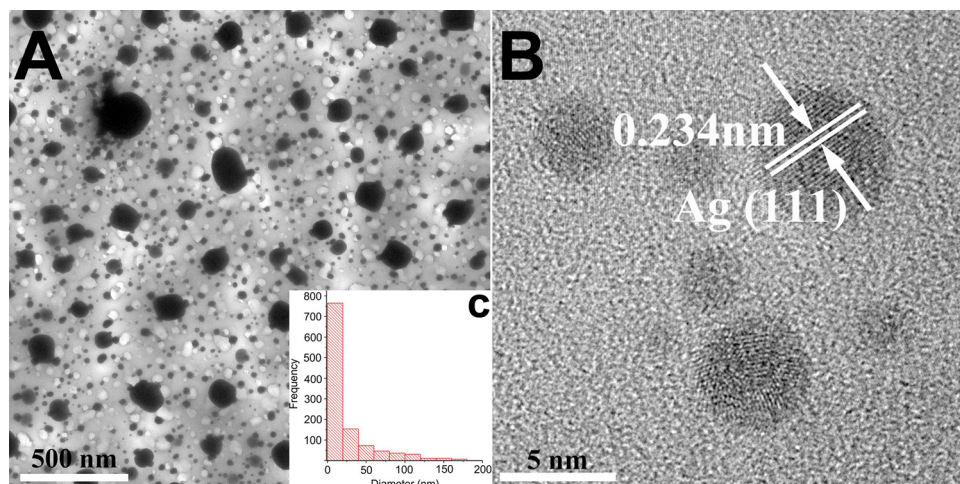


Fig. 5. TEM image (A) and high resolution image (B) of PLA + AgNO₃ coating and histogram (C) of the distribution of AgNPs in its diameters. In B the lattice stripe observed is marked.

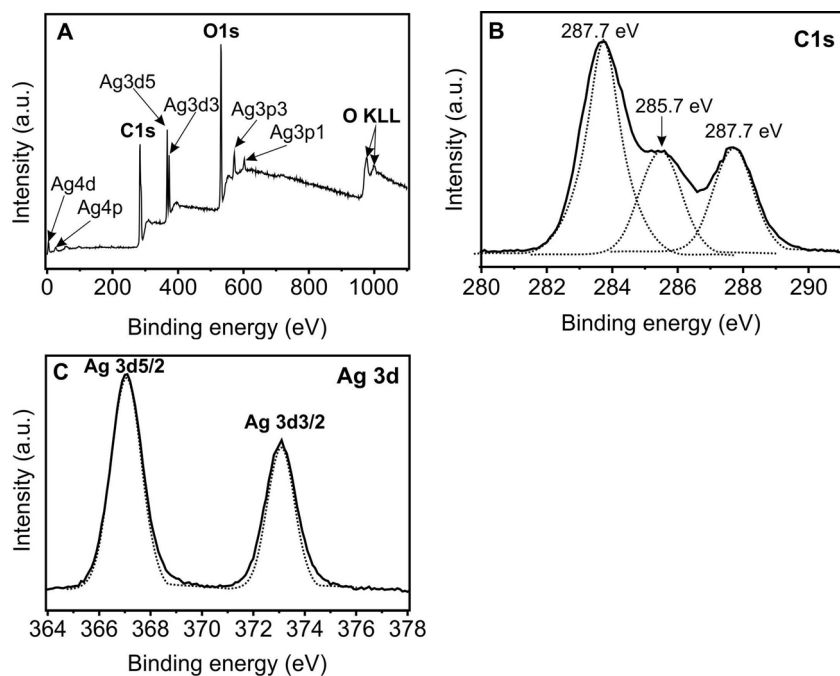


Fig. 6. XPS core spectrum (A) and XPS spectra of C 1s (B) and Ag 3d (C) of PLA + AgNO₃ coating.

initiated process are mainly considered for water solutions of the polymer and silver salt. However, the mechanism of formation of silver nanoparticles, both using aqueous solutions and for the case of electron-beam deposition, is similar. The difference lies in the mechanism of initiation of salt decomposition. At the electron-beam deposition, the salt decomposition occurs both at the stage of coating deposition (partial) and at the process of heat treatment of the already formed coating [55].

Fig. 7 presents XPS core spectrum and the XPS detailed regions of

C 1s, N 1s, and F 1s of PLA + Norfloxacin coating sample. The core XPS spectrum in Fig. 7A mainly consists of the peaks of C, N, O and F elements. C 1s XPS peaks (Fig. 7B) appear at four positions and the one of the highest binding energy at 287.6 eV can be contributed to either aliphatic C=O double bonds or F substituted aromatic carbon atoms on the benzene ring structures in Norfloxacin molecules. Besides, the other three peaks at 285.9 eV, 285.0 eV and 283.6 eV are ascribed to C atom bonded to a nitrogen atom (C–N) in Norfloxacin molecules, C–O groups and aliphatic methyl –CH₃ groups both in PLA and Norfloxacin

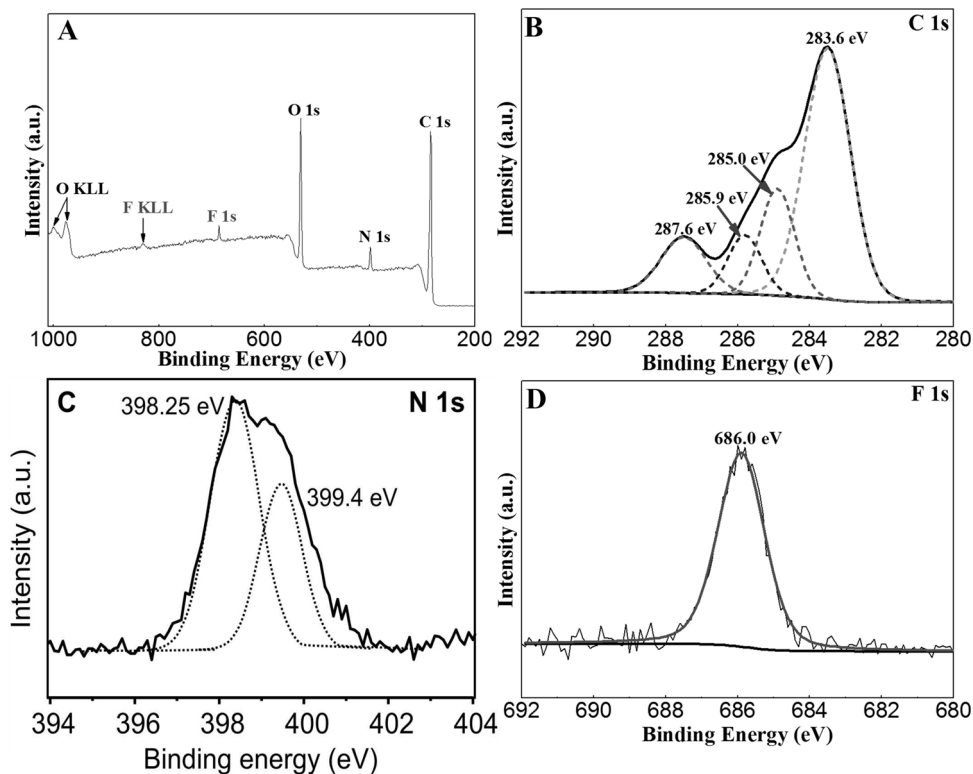


Fig. 7. XPS core spectrum (A) and XPS spectra of C 1s (B), N 1s (C) and F 1s (D) of PLA + Norfloxacin coating.

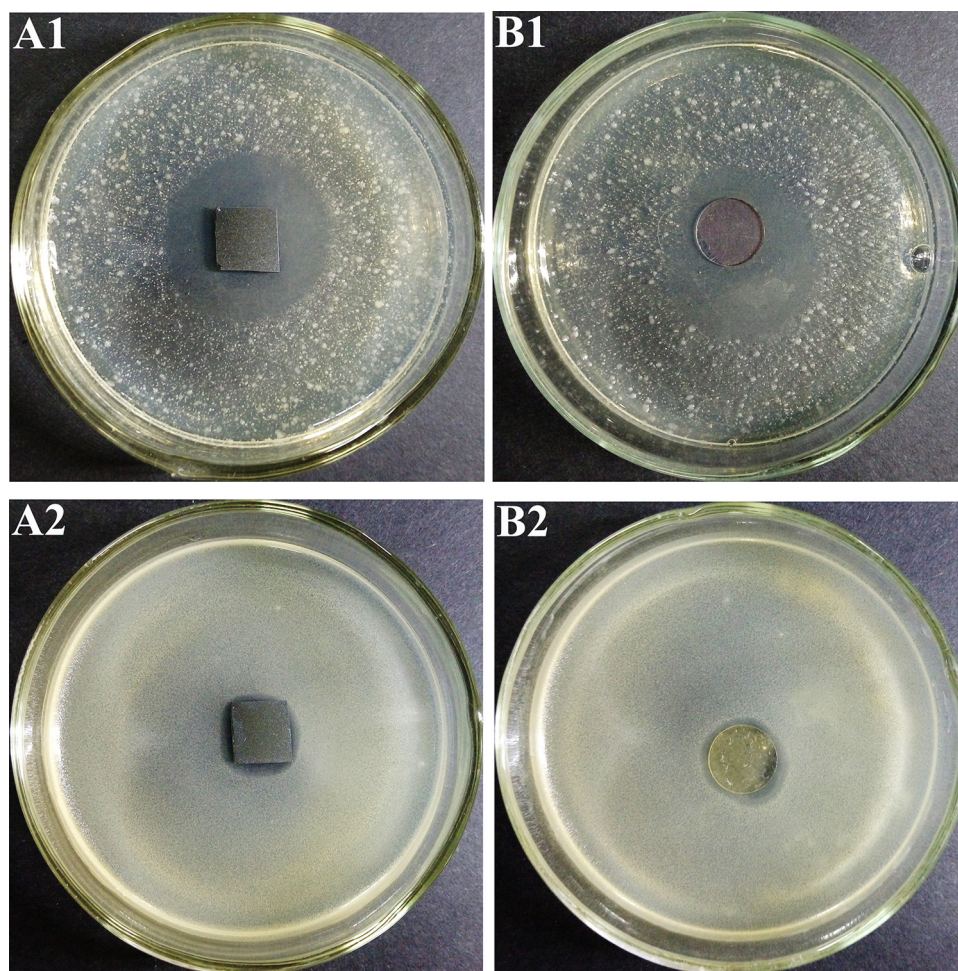


Fig. 8. Photographic images of zone of inhibition of PLA + AgNO₃ coatings deposited on different substrates (A: silicon wafers; B: quartz glasses) against *Escherichia coli* (A1, B1) and *Staphylococcus aureus* (A2, B2).

molecular structures. It clearly shows that N1s spectrum presented in Fig. 7C can be divided into two different peaks located at 399.4 eV and 398.25 eV which can be characterized to amino groups with hydrogen atoms (C)₂–N–H or N–(C)₃ groups and nitrogen atoms in a cyclic structure in Norfloxacin, respectively. The contents of the (C)₂–N–H or N–(C)₃ groups are calculated by XPS peak areas and the molar ratio of them is determined to be ca. 1:2, conform to the structure of Norfloxacin. Moreover, F1s XPS data (Fig. 7D) have only one peak centered at 686.0 eV, what allows to well determine the existence of Norfloxacin in PLA + Norfloxacin nanocomposites.

3.4. Antibacterial activity studies

The antibacterial activity of PLA-based nanocomposite coatings was investigated against pathogenic organisms *E. coli* and *S. aureus*. The visual photographic images of inhibition zones of PLA + AgNO₃ and PLA + Norfloxacin coatings are displayed in Figs. 8 and 9, respectively. All of the images of inhibition zones illustrate significant antibacterial activity of all synthesized nanocomposite coatings both against *E. coli* and *S. aureus*.

Specifically, the values of diameters in mm of inhibition zones observed from Figs. 8 and 9 are listed in Table 1. They clearly show that all PLA + Norfloxacin coating samples are more effective against both two kinds of test cultures in creating zones of inhibition with much larger areas (diameters of inhibition zones are 64.9, 56.9, 38.4 and 36.3 mm) compared to PLA + AgNO₃ samples (corresponding diameters are 26.7, 24.5, 13.4, and 12.9 mm, respectively).

The images and results of zone of inhibition also demonstrate that *E. coli* (26.7, 24.5, 64.9 and 56.9 mm) present better susceptibility to both PLA + AgNO₃ and PLA + Norfloxacin coatings in comparison with *S. aureus* (corresponding 13.4, 12.9, 38.4 and 36.3 mm). This phenomenon may be explained by their cytoplasmic membrane detachment from their cell wall under the effect of antibacterial components in the coatings [56].

As for the aspect of different substrates, it is clearly revealed that the coating samples deposited on silicon single crystal wafers (100) exhibit more obvious antibacterial activity (26.7, 13.4, 64.9 and 38.4 mm) than that on circular quartz glasses (corresponding 24.5, 12.9, 56.9 and 36.3 mm) regardless of the type of samples and the kind of cultures in these tests. It is commonly believed that the release of antibacterial components (for PLA + AgNO₃ and PLA + Norfloxacin coatings the antibacterial components are Ag nanoparticles and Norfloxacin antibiotic, respectively) determines the extent or zone of antibacterial activity as seen as the zone of inhibition [35], and this diffusion behavior can be influenced to a great extent by the substrates employed during the process of deposition of coatings for antibacterial activity studies. This explains the difference of antibacterial properties presented by the coatings on various substrates. Silver nitrate and antibacterial chemical preparation can easily diffuse into aqueous media, providing the required concentration of the drug compound near the implant. Silver nanoparticles are responsible for high surface antibacterial activity. Differences in the antibacterial activity of the compounds considered in the paper are related only to their different ability to diffuse into aqueous media. The structure of the polymer coating, its adhesion

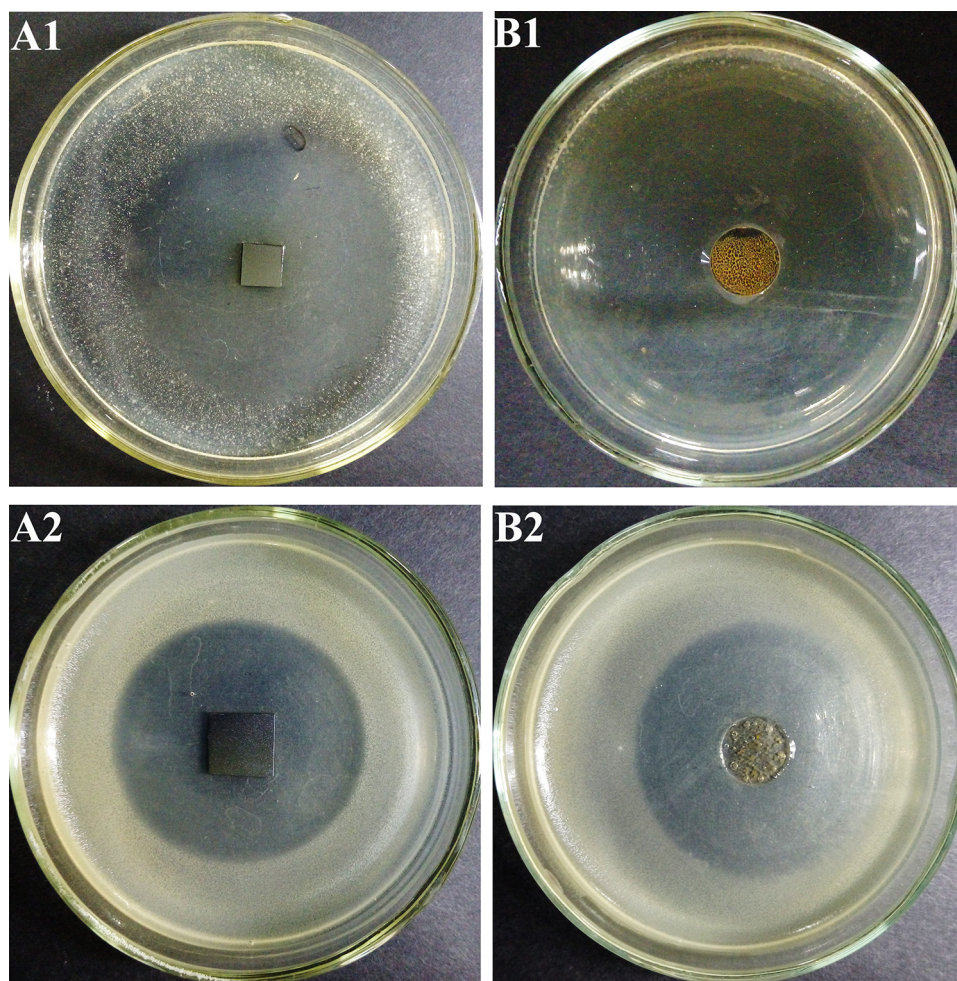


Fig. 9. Photographic images of zone of inhibition of PLA + Norfloxacin coatings deposited on different substrates (A: silicon wafer; B: quartz glasses) against *Escherichia coli* (A1, B1) and *Staphylococcus aureus* (A2, B2).

Table 1

Zone of inhibition (mm) of PLA + AgNO₃ and PLA + Norfloxacin coatings against various pathogenic organisms in terms of agar diffusion method.

Test microorganisms	Type of samples			
	PLA + AgNO ₃ coatings		PLA + Norfloxacin coatings	
	silicon wafers	quartz glasses	silicon wafers	quartz glasses
<i>E. coli</i> 25922	26.7	24.5	64.9	56.9
<i>S. aureus</i> 12600	13.4	12.9	38.4	36.3

interaction with the substrate can both facilitate and hamper the diffusion. Due to the fact that the coating is thin, its structure is significantly influenced by the substrate and, consequently, by its preliminary activation treatment. At the same time, the task was not to determine the effect of the substrate on the properties, including antibacterial, of the coatings applied. In general, all the above mentioned again confirms the effectiveness of the joint use of silver nitrate and antibacterial chemotherapy in the formation of coatings.

It should be noted then the influence of the substrate on the size of inhibition zones is shown by influencing the mechanism of the initiation and growth of the coating deposited and, respectively, through the influence on the structure of the thin layer. The processes are very complicated and require separate studies. The objectives of the paper did not include these studies. There is a considerable amount of papers

on this subject, in particular [57].

4. Conclusions

Antimicrobial PLA-based biodegradable thin nanocomposite coatings separately containing Norfloxacin and silver were successfully deposited on different substrates from the active gas phase in vacuum. The interaction between the doped antibacterial components with polymer matrix was confirmed by ATR-FTIR spectra analyses. It was found that the as-prepared PLA + Norfloxacin coatings exhibited a fine electron beam dispersion of the initial target materials as well as a good preservation of molecular structure of both PLA and Norfloxacin. In addition, the formation of AgNPs anchored on polymer matrix and the shape and size distribution of them were determined by UV-vis spectra and TEM images respectively, and their average diameter was determined to be 17.5 ± 1.13 nm. Moreover, XPS results revealed the chemical state of Ag elements and further verified the existence of metallic Ag in the case of coatings containing silver formed by electron beam dispersion of PLA and silver nitrate powder mixture. Both two kinds of PLA-based biodegradable thin coatings displayed an excellent antibacterial activity against gram-negative bacteria, *E. coli* ATCC 25922 and gram-positive bacteria, *S. aureus* ATCC 12600. And such thin nanocomposite coatings deposited on silicon single crystal wafers exhibited better antibacterial activity as opposed to them on quartz glasses. This is because of the influence of the substrates on diffusion behavior of antibacterial components in thin coating systems. Overall, this work can provide a facile path to design other organic-polymer or

metal-polymer nanocomposites which can be promising candidates applied in biomedical and biological sectors owing to their high antibacterial capacity.

Acknowledgements

This work was supported by Intergovernmental Cooperation Projects in the National Key Research and Development Plan of the Ministry of Science and Technology of PRC (projects No. 2016YFE0111800, for 2016–2019), the Belarusian Republican Foundation for Fundamental Research (project No. T16M-015, for 2016–2018), National Natural Science Foundation of China (project No. 51373077, for 2015–2016).

References

- G. Schmidmaier, M. Lucke, B. Wildemann, N.P. Haas, M. Raschke, Prophylaxis and treatment of implant-related infections by antibiotic-coated implants: a review, *Injury Int. J. Care Injur.* 37 (2006) 105–112.
- H. Vester, B. Wildemann, G. Schmidmaier, U. Stöckle, M. Lucke, Gentamycin delivered from a PDLA coating of metallic implants: in vivo and in vitro characterisation for local prophylaxis of implant-related osteomyelitis, *Injury Int. J. Care Injur.* 41 (2010) 1053–1059.
- M. Diefenbeck, C. Schrader, F. Gras, T. Mückley, J. Schmidt, S. Zankovych, J. Bossert, K.D. Jandt, A. Völpel, B.W. Sigusch, H. Schubert, S. Bischoff, W. Pfister, B. Edel, M. Faucon, U. Finger, Gentamicin coating of plasma chemical oxidized titanium alloy prevents implant-related osteomyelitis in rats, *Biomaterials* 101 (2016) 156–164.
- W.J. Metsemakers, N. Emanuel, O. Cohenb, M. Reichart, I. Potapova, T. Schmid, D. Segal, M. Riool, P.H.S. Kwakman, L. de Boer, A. de Brij, P.H. Nibbering, R.G. Richards, S.A.J. Zaat, T.F. Moriarty, A doxycycline-loaded polymer-lipid encapsulation matrix coating for the prevention of implant-related osteomyelitis due to doxycycline-resistant methicillin-resistant *Staphylococcus aureus*, *J. Control. Release* 209 (2015) 47–56.
- D.J. McMillan, C. Lutton, N. Rosenzweig, K.S. Sriprakash, B. Goss, M. Stemberger, M.A. Schuetz, R. Steck, Prevention of *Staphylococcus aureus* biofilm formation on metallic surgical implants via controlled release of gentamicin, *J. Biomed. Sci. Eng.* 4 (2011) 485–492.
- D. Pavithra, M. Doble, Biofilm formation, bacterial adhesion and host response on polymeric implants-issues and prevention, *Biomed. Mater.* 3 (2008) 3750–3756.
- I.J. Macha, B. Ben-Nissan, J. Santos, S. Cazalbou, B. Milthorpe, Hydroxyapatite/PLA biocomposite thin films for slow drug delivery of antibiotics for the treatment of bone and implant-related infections, *Key Eng. Mater.* 696 (2016) 271–276.
- M.S.S. Román, M.J. Holgado, B. Salinas, V. Rives, Drug release from layered double hydroxides and from their poly(lactic acid) (PLA) nanocomposites, *Appl. Clay Sci.* 71 (2013) 1–7.
- U. Posadowska, M. Brzyczy-Wloch, E. Pamula, Gentamicin loaded PLGA nanoparticles as local drug delivery system for the osteomyelitis treatment, *Acta Bioeng. Biomech.* 17 (2015) 41–48.
- L. Sansone, A. Aldi, P. Musto, E.D. Maio, E. Amendola, G. Mensitieri, Assessing the suitability of poly(lactic acid) flexible films for high pressure pasteurization and sterilization of packaged foodstuff, *J. Food Eng.* 111 (2012) 34–45.
- Z.Ö. Erdohan, B. Çam, K.N. Turhan, Characterization of antimicrobial poly(lactic acid) based films, *J. Food Eng.* 119 (2013) 308–315.
- P.O. Rujitanaroj, N. Pimpcha, P. Supaphol, Wound-dressing materials with antibacterial activity from electrospun gelatin fiber mats containing silver nanoparticles, *Polymer* 49 (2008) 4723–4732.
- W.A. Jiranek, A.D. Hanssen, A.S. Greenwald, Antibiotic-loaded bone cement for infection prophylaxis in total joint replacement, *J. Bone Joint Surg. Am.* 88 (2006) 2487–2500.
- A.B. Kutikov, S. Jie, Biodegradable PEG-based amphiphilic block copolymers for tissue engineering applications, *ACS Biomater. Sci. Eng.* 1 (2015) 463–480.
- I. Armentano, M. Dottori, E. Fortunati, S. Mattioli, J.M. Kenny, Biodegradable polymer matrix nanocomposites for tissue engineering: a review, *Polym. Degrad. Stab.* 95 (2010) 2126–2146.
- K. Rezwan, Q.Z. Chen, J.J. Blaker, A.R. Boccaccini, Biodegradable and bioactive porous polymer/inorganic composite scaffolds for bone tissue engineering, *Biomaterials* 27 (2006) 3413–3431.
- G. Schmidmaier, B. Wildemann, A. Stemberger, N.P. Haas, M. Raschke, Biodegradable poly(D, L-lactide) coating of implants for continuous release of growth factors, *J. Biomed. Mater. Res.* 58 (2001) 449–455.
- Y. Ramot, M.H. Zada, A.J. Domb, A. Nyska, Biocompatibility and safety of PLA and its copolymers, *Adv. Drug Deliv. Rev.* (2016).
- M. Turalija, S. Bischof, A. Budimir, S. Gaan, Antimicrobial PLA films from environment friendly additives, *Compos. Part B* 102 (2016) 94–99.
- S. Farah, D.G. Anderson, R. Langer, Physical and mechanical properties of PLA, and their functions in widespread applications – a comprehensive review, *Adv. Drug Deliv. Rev.* (2016).
- A. Nanda, M. Saravanan, Biosynthesis of silver nanoparticles from *Staphylococcus aureus* and its antimicrobial activity against MRSA and MRSE, *Nanomedicine* 5 (2009) 452–456.
- M. Ramos, E. Fortunati, M. Peltzer, A. Jimenez, J.M. Kenny, M.C. Garrigos, Characterization and disintegrability under composting conditions of PLA-based nanocomposite films with thymol and silver nanoparticles, *Polym. Degrad. Stab.* 132 (2016) 2–10.
- J.Y. Lee, Y. Liao, R. Nagahata, S. Horiuchi, Effect of metal nanoparticles on thermal stabilization of polymer/metal nanocomposites prepared by a one-step dry process, *Polymer* 47 (2006) 7970–7979.
- A.V. Rahachou, A.A. Rogachev, M.A. Yarmolenko, X.H. Jiang, Z.B. Liu, Molecular structure and optical properties of PTFE-based nanocomposite polymer-metal coatings, *Appl. Surf. Sci.* 258 (2012) 1976–1980.
- A.A. Rogachev, M.A. Yarmolenko, A.V. Rahachou, D.V. Tapalski, X.H. Liu, D.L. Gorbachev, Morphology and structure of antibacterial nanocomposite organic-polymer and metal-polymer coatings deposited from active gas phase, *RSC Adv.* 3 (2013) 11226–11233.
- P.M. Martin, *Handbook of Deposition Technologies for Films and Coatings*, third ed., Elsevier Inc., Amsterdam, 2010.
- M.A. Yarmolenko, et al., A.V. Rogachev, M. Radiotekhnika (Eds.), *Micro – and Nanocomposite Polymer Coating Deposited from Active Gas Phase*, 2016, p. 424 p.
- M.A. Yarmolenko, et al., Biocompatible Antibacterial Polymer Coatings with Ciprofloxacin Extended Release 52 *Antibiot Khimioter*, 2007, pp. 3–7.
- A. Rogachev, et al., Morphology and structure of antibacterial nanocomposite organic – polymer and metal-polymer coatings deposited from active gas phase, *RSC Adv.* 3 (2013) 11226–11233.
- LP, L.P. Krul, et al., Mechanism of formation of polylactide coatings from the active gas phase, *Doklady Natl. Acad. Sci. Belarus* 60 (2016) 72–78.
- C. Zhao, H. Wu, J. Ni, S. Zhang, X. Zhang, Development of PLA/Mg composite for orthopedic implant: tunable degradation and enhanced mineralization, *Compos. Sci. Technol.* (2017), <https://doi.org/10.1016/j.compscitech.2017.04.037>.
- Chen Qi, A.V. Rogachev, D.V. Tapalskii, M.A. Yarmolenko, A.A. Rogachev, Xiaohong Jiang, E.V. Koshanskaya, A.S. Vorontsov, Nanocomposite coatings for implants protection from microbial colonization: formation features, structure, and properties, *Surf. Coat. Technol.* 315 (2017) 350–358.
- A.V. Rahachou, M.A. Yarmolenko, A.A. Rogachev, D.L. Gorbachev, B. Zhou, Chemical composition, morphology and optical properties of zinc sulfide coatings deposited by low-energy electron beam evaporation, *Appl. Surf. Sci.* 303 (2014) 23–29.
- B. Barman, K.C. Sarma, Luminescence properties of ZnS quantum dots embedded in polymer matrix, *Chalcogenide Lett.* 8 (2011) 171–176.
- B. Bhattacharjee, D. Ganguli, K. Iakoubovskii, A. Stesmans, S. Chaudhuri, Synthesis and characterization of sol-gel derived ZnS: Mn²⁺ nanocrystallites embedded in a silica matrix, *Bull. Mater. Sci.* 25 (2002) 175–180.
- C.F. Bagamboula, M. Uyttendaele, J. Debevere, Inhibitory effect of thyme and basil essential oils, carvacrol, thymol, estragol, linalool and p-cymene towards *Shigella sonnei*, and *S. Flexneri*, *Food Microbiol.* 21 (2004) 33–42.
- D.S. Borgaonkar, E. Mules, Antimicrobial activity of essential oils from plants against selected pathogenic and saprophytic microorganisms, *J. Food Protect.* 64 (2001) 1019–1024.
- C.L. Gallant, H.Q. Yin, R.E. Langford, M.E. Olson, D.A. Hart, R.E. Burrell, 114A comparison of in vitro, disc diffusion and time-kill kinetic assays for the evaluation of antimicrobial activity of silver containing wound dressings, *Wound Repair Regen.* 12 (2004) A30-A30(1).
- A.S. Suliman, R.J. Anderson, A.A. Elkordy, Norfloxacin as a model hydrophobic drug with unique release from liquidoid formulations prepared with PEG200 and Synperonic PE/L-61 non-volatile liquid vehicles, *Powder Technol.* 257 (2014) 156–167.
- M. Zhu, P. Chen, M. Liu, Graphene oxide wrapped Ag/AgX (X = Br, Cl) nanocomposite as a highly efficient visible-light plasmonic photocatalyst, *ACS Nano* 5 (2011) 4529–4536.
- W.J. Jin, H.J. Jeon, J.H. Kim, H.Y. Ji, A study on the preparation of poly(vinyl alcohol) nanofibers containing silver nanoparticles, *Synth. Met.* 157 (2007) 454–459.
- Y.A. Akimov, W.S. Koh, K. Ostrikov, Enhancement of optical absorption in thin-film solar cells through the excitation of higher-order nanoparticle plasmon modes, *Opt. Express* 17 (2009) 10195–10205.
- S. Link, M.A. El-Sayed, Optical properties and ultrafast dynamics of metallic nanocrystals, *Annu. Rev. Phys. Chem.* 54 (2003) 331–366.
- Y. Wang, Q. Yang, G. Shan, Preparation of silver nanoparticles dispersed in polyacrylonitrile nanofiber film spun by electrospinning, *Mater. Lett.* 59 (2005) 3046–3049.
- Nakamoto, Kazuo Applications in Inorganic Chemistry[M]. *Infrared and Raman Spectra of Inorganic and Coordination Compounds: Part A: Theory and Applications in Inorganic Chemistry*, Sixth ed., John Wiley & Sons Inc., Hoboken, 2008.
- J.F. Guo, B. Ma, A. Yin, K. Fan, W.L. Dai, Highly stable and efficient Ag/AgCl@TiO₂ photocatalyst: preparation, characterization, and application in the treatment of aqueous hazardous pollutants, *J. Hazard. Mater.* 211–212 (2012) 77–82.
- E. Sumesh, M.S. Bootharaju, Anshup, T. Pradeep, A practical silver nanoparticle-based adsorbent for the removal of Hg²⁺ from water, *J. Hazard. Mater.* 189 (2011) 450–457.
- Y. Sang, L. Kuai, C. Chen, Z. Fang, B. Geng, Fabrication of a visible-light-driven plasmonic photocatalyst of AgVO₃@AgBr@Ag nanobelt heterostructures, *ACS Appl. Mater. Interfaces* 6 (2014) 5061–5068.
- N. Peng, Q. Wang, A. Zheng, Z. Zhang, J. Fan, S. Liu, J.P. Amoureux, F. Deng, Understanding the high photocatalytic activity of (B, Ag)-codoped TiO₂ under solar-light irradiation with XPS, solid-state NMR, and DFT calculations, *J. Am. Chem. Soc.* 135 (2013) 1607–1616.
- J. Lei, W. Wang, M. Song, B. Dong, Z. Li, C. Wang, L. Li, Ag/AgCl coated

- polyacrylonitrile nanofiber membranes: synthesis and photocatalytic properties, *React. Funct. Polym.* 71 (2011) 1071–1076.
- [51] Y. Yang, W. Guo, Y. Guo, Y. Zhao, X. Yuan, Y. Guo, Fabrication of Z-scheme plasmonic photocatalyst Ag@AgBr/g-C₃N₄, with enhanced visible-light photocatalytic activity, *J. Hazard. Mater.* 271 (2014) 150–159.
- [52] M.S.A.S. Shah, M. Nag, T. Kalagara, S. Singh, S.V. Manorama, Silver on PEG-PU-TiO₂ polymer nanocomposite films: an excellent system for antibacterial applications, *Chem. Mater.* 20 (2008) 2455–2460.
- [53] C. Ren, B. Yang, M. Mu, J. Xu, Z. Fu, Y. Lv, T. Guo, Y. Zhao, C. Zhu, Synthesis of Ag/ZnO nanorods array with enhanced photocatalytic performance, *J. Hazard. Mater.* 182 (2010) 123–129.
- [54] X. Hui, H. Li, J. Xia, S. Yin, Z. Luo, L. Liu, L. Xu, One-pot synthesis of visible-light-driven plasmonic photocatalyst Ag/AgCl in ionic liquid, *ACS Appl. Mater. Interfaces* 3 (2011) 22–29.
- [55] A.A. Rogachev, M.A. Yarmolenko, Xiaohong Jiang, A.V. Rogachev, Ruiqi Shen, Zhou Yingjie, Heat treatment impact on molecular structure of polymer-based silver containing coatings deposited from the active gas phase, *Prog. Org. Coat.* 81 (2015) 80–86.
- [56] Q.L. Feng, J. Wu, G.Q. Chen, F.Z. Cui, T.N. Kim, J.O. Kim, A mechanistic study of the antibacterial effect of silver ions on *Escherichia coli*, and *Staphylococcus aureus*, *J. Biomed. Mater. Res.* 52 (2000) 662–668.
- [57] A.A. Rogachev, M.A. Yarmolenko, A.V. Rogachev, Growth peculiarities and molecular structure of polytetrafluoroethylene coatings deposited from an active gas phase on activated surface, *J. Surface Invest. X-Ray, Synchrotron Neutron Tech.* (2010) 39–43.